Composites Science and Technology 69 (2009) 228–238

Contents lists available at ScienceDirect

Composites Science and Technology

journal homepage: www.elsevier.com/locate/compscitech

A novel image analysis procedure for measuring fibre misalignment in unidirectional fibre composites

K.K. Kratmann [a,c,*], M.P.F. Sutcliffe [b], L.T. Lilleheden [c], R. Pyrz [a], O.T. Thomsen [a]

[a] Department of Mechanical Engineering, Aalborg University, Pontoppidanstræde 101, DK-9220 Aalborg, Denmark
[b] Department of Engineering, University of Cambridge, Trumpington Street, Cambridge, CB2 1PZ, UK
[c] Fiberline Composites A/S, Barmstedt Allé 5, DK-5500 Middelfart, Denmark

ARTICLE INFO

Article history:
Received 5 March 2008
Received in revised form 3 October 2008
Accepted 13 October 2008
Available online 5 November 2008

Keywords:
A. Carbon fibres
A. Polymer–matrix composites
B. Strength
D. Optical microscopy
E. Pultrusion

ABSTRACT

A novel image analysis procedure named Fourier transform misalignment analysis (FTMA) for measuring fibre misalignment in unidirectional fibre composites is presented. Existing methods are briefly illustrated and evaluated. The FTMA-method is presented, describing the specimen preparation and elaborating how the image analysis algorithm uses Fourier transformation and a least squares method to compute single fibre orientations. On the basis of parameter investigations the robustness of the FTMA-method is investigated. Software generated micrographs with known fibre misalignment are used to determine the precision of the method. The precision is used, along with computation time and memory usage, to benchmark the FTMA-method against the existing multiple field image analysis (MFIA) method. It is found that the FTMA-method is at least as accurate as existing methods. Furthermore, the FTMA-method is much faster than the existing methods, completing a typical analysis in approximately 1 min. Overall, it is concluded that the FTMA-method is a robust, precise and time efficient tool for determining fibre misalignment in unidirectional fibre composites, offering a higher degree of detail than the existing MFIA-method.

1. Introduction

During the last decade the use of carbon fibre reinforced plastics (CFRP) has spread from aerospace industry to a wide range of industrial applications including bridge reinforcements, wind turbine blades, automotive and marine/offshore. Large quantities of relatively expensive CFRP are being used in these industry sectors, so that the material performance relative to its cost has become a key factor. There is therefore a high motivation for improving the performance of the very expensive CFRP composites.

One material property of specific interest is the compressive strength, which in most commercial unidirectional CFRPs is about 50% of the tensile strength [1]. This often makes the compressive strength one of the limiting design factors in large composites structures.

It is widely accepted that the dominant failure mode in most commercial unidirectional polymer–matrix fibre composites is plastic microbuckling [1,2]. In the early models of microbuckling failure in unidirectional fibre composites the fibre misalignment was identified as one of the main governing properties. The fibre misalignment is a geometric material imperfection which is closely linked to the production method. The other governing properties are the shear modulus and the shear yield strain of the composite and therefore closely linked to the choice of materials.

Fiberline Composites, a manufacturer of pultruded composite profiles, has through Aalborg University, Denmark, initiated the development of a time efficient tool for quantification of fibre misalignment. Fiberline Composites aims to use such a tool in the development of future, high performance, fibre composites. In general a fast and precise tool for measuring fibre misalignment in composite materials will be of value:

- To the manufacturer trying to improve manufacturing techniques.
- In quality control, giving a fast estimate of the compressive strength.
- To engineering scientists wanting precise input for further development of compressive strength models.

Yurgartis [3] proposed a sectioning technique using classic 2D optical reflection microscopy. The basic idea is that fibres of circular cross-section appear as ellipsoids when sectioned on a plane inclined at an angle to the nominal fibre direction. By measuring the major and minor axes of such ellipsoids the orientation of the fibres can then be derived. This technique requires high quality

* Corresponding author. Address: Department of Mechanical Engineering, Aalborg University, Pontoppidanstræde 101, DK-9220 Aalborg, Denmark. Tel.: +45 25 27 76 42; fax: +45 70 13 77 14.
E-mail address: kkr@fiberline.com (K.K. Kratmann).

0266-3538/$ - see front matter © 2008 Elsevier Ltd. All rights reserved.
doi:10.1016/j.compscitech.2008.10.020

polishing along with high magnification micrographs. Moreover, it is sensitive to irregular fibre shapes and it is relatively time consuming.

Non-destructive methods such as described by Clarke et al. [4,5] have been proposed, where confocal laser scanning microscopy (CLSM) is used to determine the fibre misalignment. However such methods are not applicable to CFRP, due to the opacity of carbon fibres. Creighton et al. [6] proposed the multiple field image analysis (MFIA) method. The MFIA-method uses digital micrographs of planes sectioned parallel to the nominal fibre direction, where fibres appear as elongated features. The MFIA-method was faster than existing methods both in regard to specimen preparation and analysis time. Nevertheless, analysis time for a typical analysis was reported to take 3 h [6] and the precision of the method was not fully investigated.

Digital image analysis is a discipline which has been implemented with success in various fields such as cell biology, surveillance, radiology and quality control, etc. Typical tasks undertaken in image analysis are filtering, pattern recognition, counting and measuring; appropriate algorithms can be made extremely time efficient. Many standard tools for image analysis have been developed and can be explored with the freeware program ImageJ [7], among others. The method proposed in this paper is named Fourier transform misalignment analysis and will from here on be referred to as the FTMA-method. The FTMA-method utilises 2D Fourier transformation as the key image analysis algorithm, which decomposes digital images into frequency and intensity components. If a repetitive pattern exists in a picture it will show up in the frequency domain of a 2D Fourier transformation [8]. An appropriate frequency filter can enhance such patterns.

The FTMA-method is similar to the MFIA-method, analysing digital micrographs of section planes parallel to the nominal fibre direction of unidirectional CFRP. In such planes the fibres are found in repetitive patterns of orientation and spacing. A frequency filter designed to enhance the fibre pattern through 2D Fourier transformation of digital micrographs has been designed. The frequency filter has been included in a new image analysis algorithm especially designed to enable time efficient measurement of fibre misalignment. Using real micrographs of unidirectional CFRP the design parameters of the frequency filter have been investigated and shown to exert little influence on the computed result. The precision of the method has been investigated on software generated micrographs, and the method has been benchmarked against the MFIA-method for time efficiency and memory usage.

2. Analysis methods

2.1. Modelling of compressive failure due to microbuckling in unidirectional composites

Rosen [9] is generally known as the first to describe compressive failure of unidirectional fibre composites as elastic microbuckling. He gathered results from earlier studies including photo elastic experiments. In the photo elastic experiments single fibres were embedded in a matrix and compressed by cooling which resulted in repetitive sinusoidal deformation. These experiments were used to demonstrate that the treatment of compressive failure as buckling of columns resting on an elastic foundation is valid also for brittle materials such as glass. Conceptually, two different elastic modes are possible. The fibres will buckle either in phase, where the matrix undergoes shear, or out off phase with the matrix being in tension–compression as shown in Fig. 1.

The in-phase phase mode with the matrix loaded in shear has the lower buckling stress. Assuming that the fibres are perfectly aligned the elastic buckling stress is expressed as

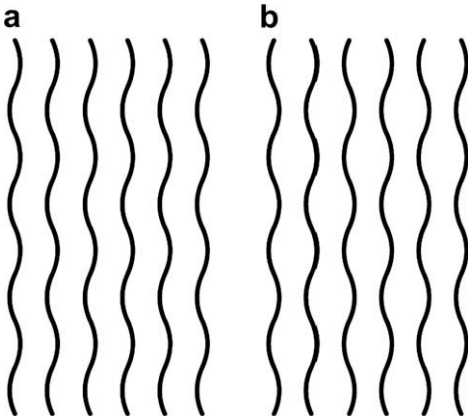

Fig. 1. Sketch of the elastic buckling modes of continuous fibres in compression described by Rosen [9]. (a) In-phase buckling with the matrix in shear. (b) Out-of-phase buckling with the matrix in compression–tension.

$$\sigma_c = G \tag{1}$$

where G is the effective longitudinal shear modulus of the composite. Originally the effective shear modulus was estimated by taking the matrix shear modulus acting over the matrix volume fraction.

Today it is widely accepted that the dominant compression failure mode in most commercial unidirectional polymer–matrix fibre composites is localised plastic microbuckling [1,2,10–12].

Argon [13] suggested that the elastic model of Rosen [9] represents an upper bound for perfectly aligned composites and pointed out that composites made by normal production techniques always have regions with misaligned fibres. Modelling the initial fibre misalignment as an infinite kink band, as shown in Fig. 2, he suggested a rigid-perfectly plastic model expressed as [13]

$$\sigma_c = \frac{k}{\phi_0} \tag{2}$$

Here k is the longitudinal shear yield strength and ϕ_0 is the initial fibre misalignment angle. Further rotation of the kink band will not develop until the critical stress σ_c is reached.

Budiansky [14] extended Argon's model to an elastic-perfectly plastic model where the critical kinking stress

$$\sigma_c = \frac{G}{1 + \phi_0/\gamma_Y} \tag{3}$$

is governed by the composite shear modulus G, the shear yield strain γ_Y and the initial fibre misalignment ϕ_0. It is seen that this elastic-perfectly plastic model will reduce to Rosen's elastic model

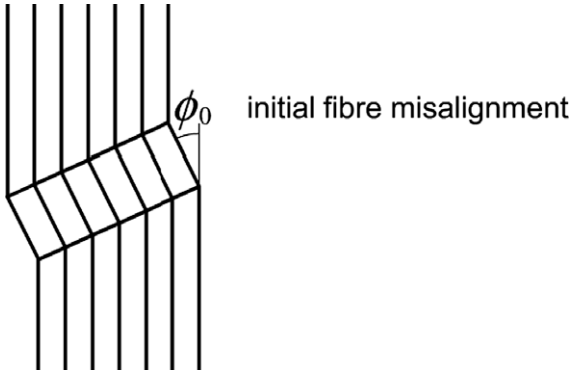

Fig. 2. Infinite kink band with initial fibre misalignment [13].

by taking the limit of $\phi_0 \to 0$. It can also be reduced to Argon's rigid plastic model by using $k = G\gamma_Y$ and taking the limit of $\gamma_Y \to 0$.

More recently the elastic-perfectly plastic model has been extended to include strain hardening and finite fibre bending resistance [1,2], while still treating the initial fibre misalignment as an infinite kink band. The infinite kink band models are often thought of as providing lower bounds of the "true" compressive strengths as they are often in good agreement with test results from pure compression tests [11]. However, as Wisnom [15] described, this test method in itself is sensitive to uniform misalignment with respect to the loading axis. Numerous finite element studies [11,16,17] have therefore been carried out to investigate sensitivity to the geometric characteristics of misalignment imperfections. Resent research by Liu et al. [18] allows the prediction of the statistical distribution of the compressive strength based on random distributions of fibre misalignment and concludes that the compressive strength mainly depends on the root mean square of the fibre misalignment.

2.2. Illustration and evaluation of existing methods for the estimation of fibre misalignment

The Yurgartis method [3] is a cross-sectional method using classical 2D optical microscopy. The basic idea behind the method is that a fibre of circular cross section will appear as an ellipsoid when sectioned in a selected angle to the nominal fibre direction as illustrated in Fig. 3.

By measuring the major and minor axes of the ellipsoids and knowing the fibre diameter the 3D spatial orientation of the fibres can be estimated. Yurgartis suggests a sectioning angle of approximately 5° to the nominal fibre orientation, where the fibre orientation can be determined with a resolution of ±0.25° [3]. The measurements can be fully automated with standard image analysis software. The specimen preparation, however, remains relatively difficult and time consuming. The reason for this is that a high polishing quality is necessary to avoid polishing artefacts that will complicate the measurement of the major axis. Furthermore, several test samples need to be polished and analyzed in order to obtain a sufficient statistical background. An example of a sectioned, polished specimen is shown in Fig. 4.

Another disadvantage of the Yurgartis method is its sensitivity to fibre shape. Not all fibres are circular. Fibres can for instance be polygonal or kidney shaped. In such cases the Yurgartis method is not applicable and other methods must be considered.

Multiple field image analysis (MFIA) is an image analysis software which was proposed by Creighton et al. [6]. With this method surfaces parallel to the fibre direction are observed. In these planes the fibres appear as elongated features as shown in Fig. 3. The MFIA software algorithm analyses local domains of a micrograph and determines the average fibre orientation by tracking intensity variations. A digital micrograph taken at relatively low magnification is

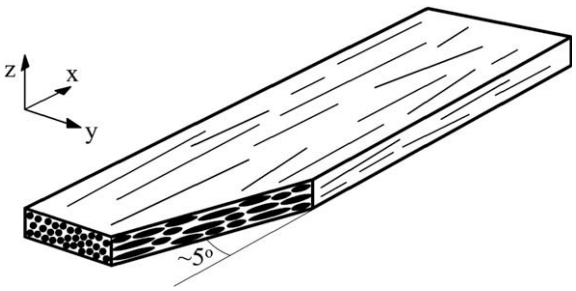

Fig. 3. Sketch showing a unidirectional composite with the nominal fibre direction being parallel to the *x*-direction.

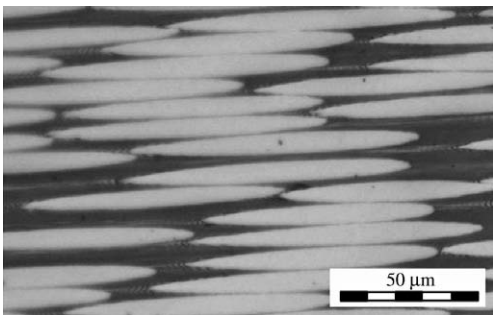

Fig. 4. Micrograph of a polished cross-sectional cut at an angle of ~5° to the nominal fibre direction of a unidirectional CFRP laminate manufactured by pultrusion.

divided into several domains as shown in Fig. 5. The domains contain several interpolation arrays which are rotated in a step-wise manner to compute the intensity variation as a function of orientation.

Fig. 6 shows that the intensity variation is closely connected to the angle at which the intensity is computed. The more parallel the interpolation is array to the fibre orientation the smaller is the intensity variation. The average orientation of each domain is determined as the angle at which the intensity variation is smallest and stored for subsequent statistical analysis. Because the micrographs are captured at a relatively low magnification (100×) a low polishing quality is sufficient, and a significant amount of time can be saved preparing the specimens, as compared to the Yurgartis method. However, the original MFIA-method is relatively time consuming, and a typical fibre misalignment analysis originally reported to take 3 h [6] is estimated to take approximately 15 min on a 1.86 GHz Pentium M processor with 1.5 GB RAM.

As a part of the present study a modified MFIA-method has been developed and made more efficient in terms of computation time. The main difference between the original and the modified version is that all domains are now rotated and analysed simultaneously. The computation time is thereby reduced to a few minutes (see Section 3.2). The "price" paid for the increased time efficiency is increased memory usage, because all the domain analyses are performed simultaneously.

A general disadvantage of the MFIA-method is that it computes average orientations, and a "true" measure of the random misalignment within the domains cannot be obtained. Furthermore, it is difficult to visually control whether a computed orientation is a good match for the local fibre orientation. This can be seen

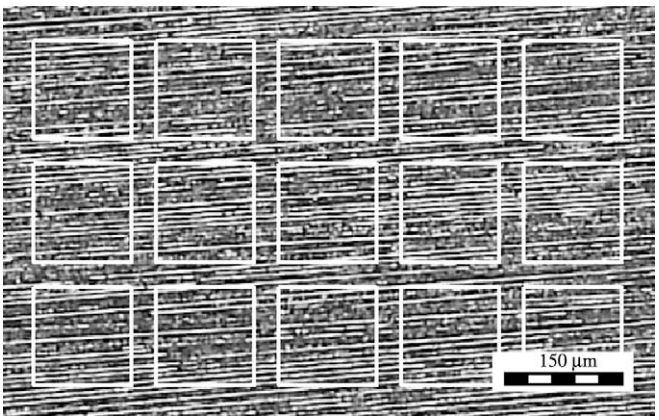

Fig. 5. Micrograph of pultruded carbon fibres captured at 100× magnification. The domains outlined in white have an edge length of 80 pixels.

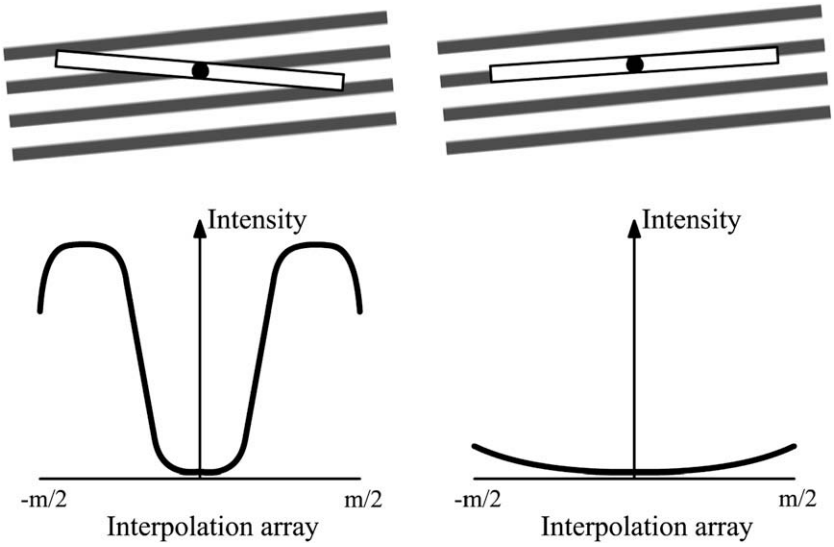

Fig. 6. Intensity distributions along two interpolation arrays with different angles relative to the fibre orientation. The more parallel an interpolation array is to the fibre orientation the smaller is the intensity variation.

in Fig. 7 where a result plot from the improved MFIA-method is shown.

Another disadvantage of the MFIA-method is that the method is sensitive to surface scratches which give a low intensity variation in the direction of the scratches and thereby distort the measurements. The modified MFIA-method described in Section 3.2 will be compared to the FTMA-method regarding precision, analysis time and memory usage.

2.3. Novel method for fibre misalignment analysis

The FTMA-method proposed in this paper for the measurement of the fibre misalignment in unidirectional composites is a digital image analysis procedure developed in MatLab®. In a similar approach to the MFIA-method [6], it works on planes parallel to the nominal fibre orientation in which fibres appear as elongated features. Such planes could be the *xy*- or *xz*-planes as shown in Fig. 3. In these planes the single fibres can be distinguished from each another at much lower magnification than with the Yurgartis method. This requires less specimen preparation and large regions can easier be analysed, giving more information regarding the distribution of fibre misalignment per micrograph than with the Yurgartis method.

2.3.1. Specimen preparation

The focus has been on developing a method which is simple and very easy to work with. A fast specimen preparation procedure which consists of two simple steps has therefore been used:

1. The specimen is wet ground down to the plane of interest with a 320 grit SiC paper. It is recommended that a grinding fixture is used to improve the parallelism of the ground plane relative to the nominal fibre orientation and to minimise rounding of the corners.
2. The coarse grind will leave a relative coarse surface with fibres sticking out of the surface which will distort the image acquisition. To remove the loose fibres the specimen is subsequently wet ground by hand a few times parallel to the fibre direction using a 1000 grit SiC paper. The specimen is now ready for image acquisition.

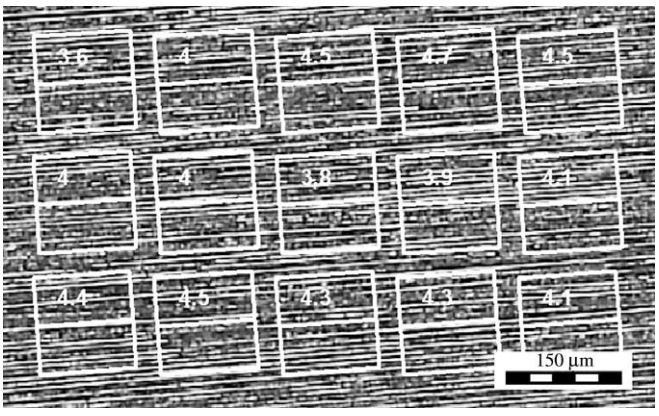

Fig. 7. Control plot from the improved MFIA-method. Each of the domains is rotated by the mean fibre orientation angle of the domain. The estimated orientation angle is written within the domain box.

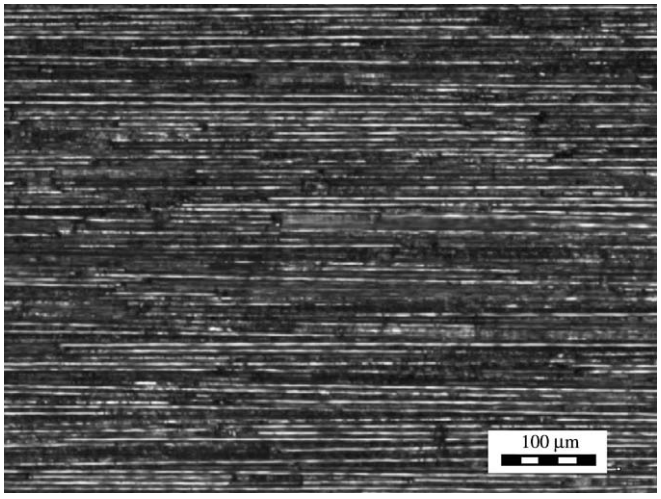

Fig. 8. Micrograph of pultruded CFRP specimen prepared with the suggested procedure.

A micrograph captured at 100× magnification of a specimen prepared with the above procedure is shown in Fig. 8.

As seen in Fig. 8 the proposed specimen preparation is relatively coarse, but as will be shown it is sufficient for performing a misalignment analysis with the FTMA-method.

2.4. Step-by-step description of the proposed image analysis algorithm

2.4.1. Step 1: performing 2D fast Fourier transformation and computing the power spectrum

The micrograph is divided into several square domains as with the MFIA-method, see Fig. 5. Each domain is represented by a matrix of pixels with 8-bit greyscale intensities. Such a domain matrix represents the spatial domain $f(x,y)$. The spatial domain is then transformed into the frequency domain denoted $F(u,v)$ using a 2D fast Fourier transformation (FFT), which is available as a built-in function "fft2" in MatLab.

To interpret the frequency domain computed by the FFT the power spectrum $P(u,v)$ is computed as

$$P(u,v) = abs(F(u,v)) = [R^2(u,v) + I^2(u,v)]^{1/2} \quad (4)$$

where $I(u,v)$ and $R(u,v)$ represent the real and imaginary parts of the Fourier coefficients. However, the dynamic range of the power spectrum is often very large as compared to an 8-bit greyscale. A logarithmic transformation is therefore used to scale the power spectrum and is computed as

$$P_{\ln}(u,v) = \ln(1 + P(u,v)) \quad (5)$$

Because of the periodic properties of the Fourier transformation the largest intensities in the frequency domain are placed in the corners. For subsequent analysis the power spectrum needs to be centred. This is done by shifting the 4-quarters in the frequency domain in accordance with Fig. 9.

This centring of the Fourier domain is performed using the built-in MatLab function called "fftshift". The three operations in obtaining a centred logarithmic power spectrum from a micrograph domain are illustrated in Fig. 10. The orientation of the fibres gives a repetitive change from black to white traversing perpendicular to the fibre direction, as shown in Fig. 10. This pattern results in a white line in the centred power spectrum shown encircled by an ellipse in Fig. 10. The next step is to determine the orientation of this white line.

2.4.2. Step 2: determination of average fibre orientation from Fourier power spectrum

The encircled white line in the power spectrum seen in Fig. 10 represents the averaged fibre orientation within the analysed domain. Determination of this mean fibre orientation is needed to build a domain-specific frequency filter. The orientation of the white line is determined by looping through the angles from 0° to 180° in steps of 0.1°. At each angle increment the radius vector of the inscribed circle, shown in Fig. 11, is drawn in the specified angle, intensities interpolated along it and summarised.

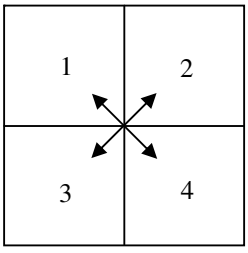

Fig. 9. Sketch of how the four quarters of the power spectrum are shifted so the largest intensities of the Fourier domain are centred.

The summation along the radius vector of the interpolated pixel intensities can be expressed as

$$P_{\text{sum}}(\theta) = \sum_{L=1}^{N/2} P_{\ln}(N/2 + \cos\theta \cdot L, N/2 - \sin\theta L) \quad \theta\varepsilon[0:0.1:180] \quad (6)$$

The orientation of the white line is determined as the angle with the highest intensity sum.

2.4.3. Step 3: domain-specific frequency filter, filtering and inverse FFT

A domain-specific filter has been designed to improve the analysis accuracy. The filter, of the same size as the domain, is illustrated in Fig. 12, showing two white regions at the fibre orientation estimated from the previous step symmetrically placed with respect to the centre. White denotes a filtering value of one, black is zero and greyscales are scalars in between. By aligning the white regions with the mean fibre orientation the filter enhances the fibre pattern and removes any noise and patterns not in that general direction. The distance between the two white regions in the centre of the image is defined as two times the filter radius.

To avoid so-called ringing effects [8] when returning to the spatial domain, ideal filters as shown in Fig. 12a should be avoided. To smooth the transition from white to black in the filter the Butterworth equation given below is used

$$G^2\omega = \frac{G_0^2}{1 + (\omega/\omega_c)^{2n}} \quad (7)$$

where G is the gain; G_0 is the gain at zero frequency; n is the order of the filter; ω is the frequency/distance to the centre and ω_C is the cut-off frequency/distance where the gain is a factor of $1/\sqrt{2}$. The Butterworth parameters are illustrated in Fig. 13.

The filter shown in Fig. 12b is built for a domain of 200 by 200 pixels with a filter radius of 20 pixels, an order of $n = 3$, and a cut-off distance of six pixels. These parameters are found to give accurate and robust results. The order of the Butterworth filter, the cut-off distance and the filter radius will be the focus of a parameter study in Section 2.5, investigating the robustness of the FTMA-method. This filter is applied to the frequency domain with element-by-element multiplication. A filtered spatial domain is then obtained by performing an inverse FFT. The result of such a filtering and inverse Fourier transformation is shown in Fig. 14.

2.4.4. Step 4: thresholding and object filtering

The filtered spatial domain is converted to a binary representation by simple thresholding, and the resulting regions are labelled using 8-node connectivity. As seen in Fig. 15a not all noise is removed by the frequency filter. An object filter is therefore used. An early version of the object filter was based on area and compactness of the objects, but the present versions of the object filter are based on the object length as it has shown to make the area and compactness thresholds redundant. The threshold of the object length is set to 25% of the domain length based on experience. All objects shorter than that are removed. The effect of the object filter is shown in Fig. 15b. If the frequency filtering is not performed a significant amount of noise joins the fibre objects and distorts further analysis, as seen in the images without filtering shown in Fig. 15c and d.

2.4.5. Step 5: computing object orientation by least squares method

The final loop in the FTMA-method computes the orientation of the resulting objects, see Fig. 15b. One object at a time coordinate sets (x_n, y_n) of all n pixels in an object are obtained. The object orientation is then determined by linear regression using the least squares method. The regression line has the form

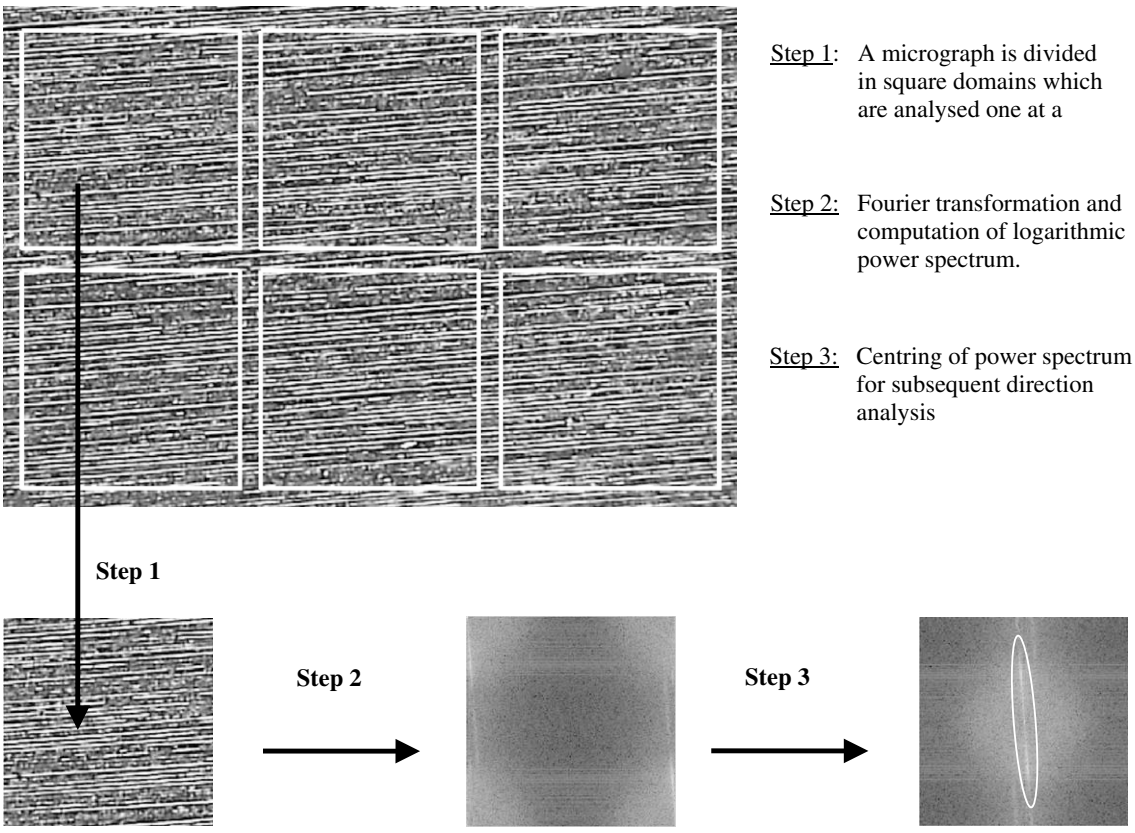

Fig. 10. An illustration of the three operations used to obtain a centred logarithmic power spectrum from a squared micrograph domain.

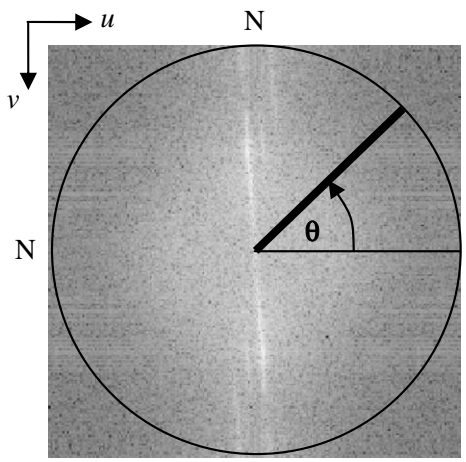

Fig. 11. Centred power spectrum with illustration of the radius vector used to determine the orientation of white line which is perpendicular to the mean fibre orientation.

$$\alpha x + \beta = y \tag{8}$$

where the line coefficients are determined as

$$\beta = \frac{nS_{XY} - S_X S_Y}{nS_{XX} - S_X S_X} \quad \alpha = \frac{S_Y - \beta S_X}{n} \tag{9}$$

$$\begin{aligned} S_X &= \sum_{i=1}^{n} x_i \quad S_{XX} = \sum_{i=1}^{n} x_i^2 \\ S_Y &= \sum_{i=1}^{n} y_i \quad S_{XY} = \sum_{i=1}^{n} x_i y_i \end{aligned} \tag{10}$$

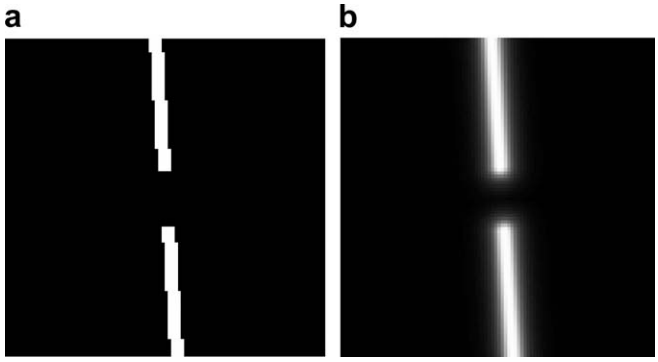

Fig. 12. Filter with two areas placed symmetrical with respect to the centre and aligned with the mean fibre orientation. (a) Ideal black and white filter. (b) Transition from white to black smoothed with the Butterworth equation.

When an orientation for all the objects within a domain is determined, it is possible to have the computed regression lines plotted on the active domain as shown in Fig. 16.

The mean orientation and standard deviation within the domain is computed and stored along with the single object orientations for subsequent statistic analysis. The misalignment analysis then moves on to the next domain.

2.5. Robustness

Micrographs of different CFRP specimens have been used in a thorough parameter study. The focus has been on the filter radius, power and cut-off distance of the frequency filter. The robustness has then been investigated by observing how the parameters influence the analysis result. More specifically, each parameter has

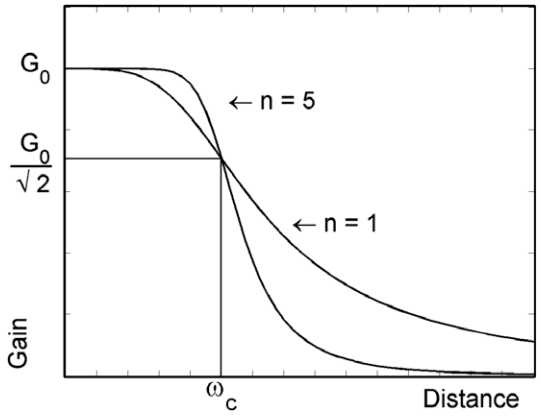

Fig. 13. Illustration of the Butterworth equation and its parameters.

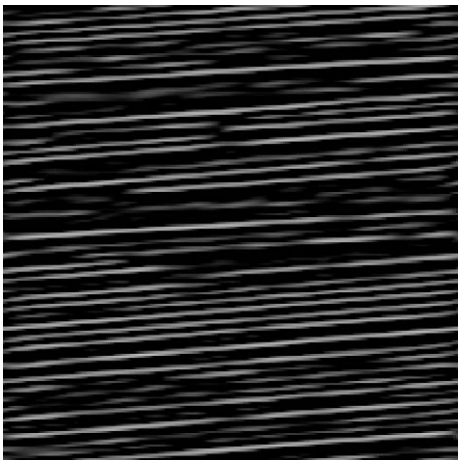

Fig. 14. Filtered spatial domain with enhanced fibre pattern obtained by inverse FFT of the filtered frequency domain.

been assigned four different values which have been varied independently giving 64 analyses per investigation. For each variation the mean angle and standard deviation has been computed and stored for later comparison. Twelve domains representing three different materials have been investigated. Parameter investigations have also been performed on software generated micrographs to check that such analyses gave the similar results. Finally, visual control plots as shown in Fig. 16 have been used for comparison of the different results in a parameter investigation. Selected results from the parameter study are given and discussed in Section 3.1.

2.6. Precision and benchmarking

Software generated micrographs have been used to determine the precision of the FTMA-method. A software generated micrograph, as shown in Fig. 17, has the advantage that the orientation of every drawn fibre is known as well as the mean orientation and standard deviation. The software generated micrographs are constructed by generating normal distributions of fibre orientations and fibre lengths with defined mean and standard deviation. Each fibre position is obtained from a uniform distribution of coordinates within the image area. Each fibre is then evaluated in turn against a set of rules designed to avoid fibre crossing and fibres lying to close. If the potential fibre does not violate any of the rules, it is plotted on the image and the next fibre is evaluated. Finally, noise is added to the image to enhance the resemblance to real fibre patterns.

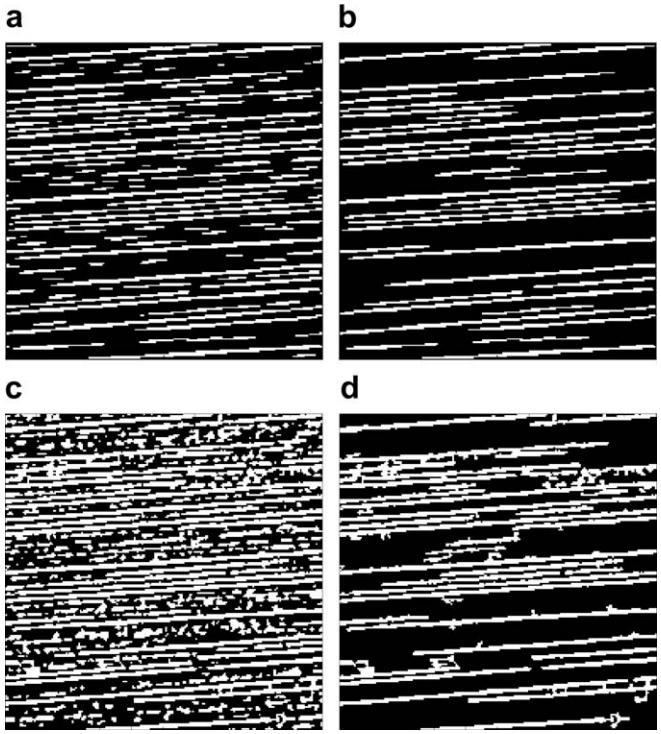

Fig. 15. Thresholded images of the spatial domain. (a) Frequency filtered, no object filtering. (b) Frequency filtered, object filtering on the basis object length. (c) No frequency filtering, no object filtering. (d) No frequency filtering, object filtering on the basis of object length.

By performing a misalignment analysis with several domains the mean orientation and standard deviation can be estimated on a given image. The precision will then be computed as the difference between the known and measured value of the mean orientation and standard deviation.

The benchmark covers precision, computational time efficiency and memory usage. The benchmarking of the precision is carried out on software generated micrographs. Benchmarking of the computation time and memory usage is carried out by varying the analysis size on a typical micrograph of unidirectional CFRP.

3. Results

3.1. Robustness

The robustness of the FTMA-method has been investigated on several micrographs with the focus on how the filter parameters influence the computed results with respect to both mean orientation and standard deviation. The results of a typical parameter investigation regarding mean orientation from one domain are shown in Fig. 18. Parameter investigations on software generated micrographs produce more consistent results. The overall response is nevertheless the same as compared to real micrographs. By using the visual control plots, in combination with parameter investigation on the real micrographs, the following conclusions can be reached. Filter radii of 0, 10, 20 and 40 pixels have been used on 200×200 pixel domains. A small filter radius of 0 or 10 pixels lets too much noise slip through the frequency filter and tends to generate bridges between independent fibre segments which disturb the result. Using a large filter radius of 40 pixels on the other hand tends to generate "echo objects" in the gap between fibres. Neither of these analysis artefacts has been observed with a filter radius of 20 pixels, which is therefore recommended as the standard filter radius. Nevertheless, little difference is observed regarding the re-

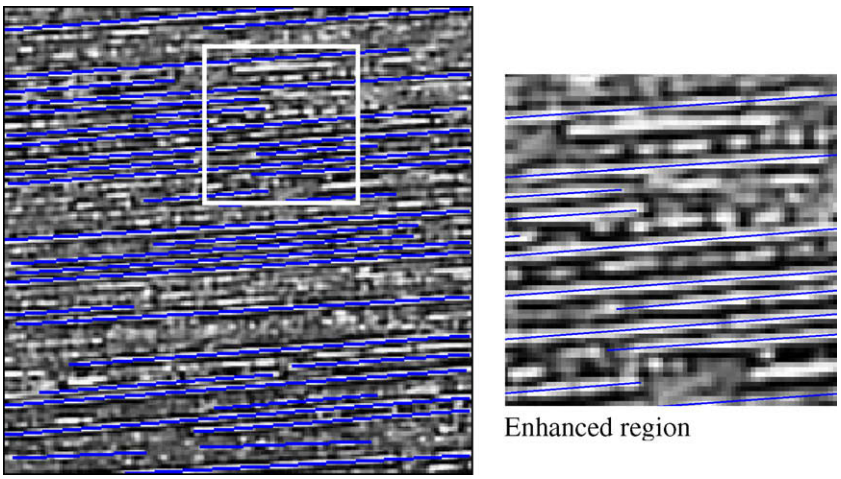

Fig. 16. Results plot from the FTMA-method for visual control of the computed regression lines.

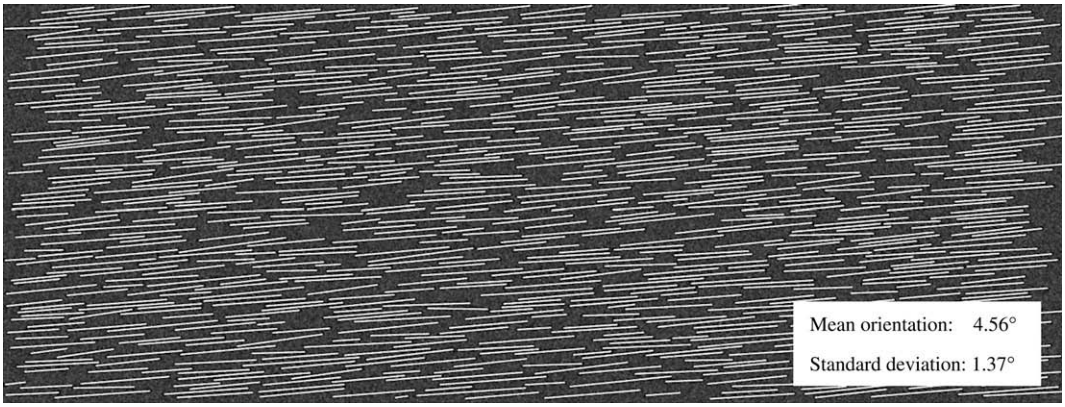

Fig. 17. Software generated micrograph where the orientation of every drawn fibre is known.

sults. This is supported by Fig. 18 which shows that the computed mean orientation lies between approximately 4.1° and 4.4° regardless of the filter parameters.

Cut-off distances of 1, 2, 5 and 10 pixels and filter orders of $n = 1$, 2, 3 and 5 have been used in the parameter study. The cut-off distance, together with the filter order, controls the width of the filter and thereby the orientation interval which is isolated and enhanced. A narrow filter ignores objects whose orientation deviate too much from the mean orientation. A narrow filter also tends to build bridges between independent fibre segments. Extreme cases of such filter behaviour can be seen when analysing software generated micrographs as shown in Fig. 19.

The sensitivity to the cut-off distance and filter order is significantly smaller when the parameter investigations are performed on real micrographs of CFRP. The parameter study shows that with a filter radius of 20 pixels and a cut-off distance equal to or above 5 pixels all parameter investigations compute mean orientations that are consistent within ±0.2°, often with better consistency than this.

With regard to robustness of the computed standard deviation the results are not always consistent. When computing the standard deviation, results consistent within ±0.3° are observed in 2 out of 12 parameter investigations. One of these is shown in Fig. 20a. The larger variation can be explained by poor contrast in some of the analysed micrographs.

An example of a parameter investigation with consistent results is shown in Fig. 20b. Such results can be explained by good contrast in the analysed micrograph, which again can be related to a better (though still relatively coarse) polishing quality. The consistent results seen in Fig. 20b are similar to the parameter investigations of software generated micrographs, where the variation of the computed standard deviation are within ±0.1° for a cut-off distance above 1 pixel.

Regarding the filter order it is recommended to use $n = 3$. A higher filter order results in a filter design, close to an ideal filter, which according to literature introduces filtering artefacts [8]. This complies with observations indicating that the high order filter, $n = 5$, gives less consistent results, however still within ±0.2° regarding mean orientation. Using a lower order of $n = 2$ has in general little (if any) influence on the results. Using an order of $n = 1$ is, however, too small as it makes the width of the filter too large and thereby enables noise to get through.

In summary, the parameter study shows that the robustness of the FTMA-method is satisfactory as the computed mean orientations are consistent within ±0.2° regardless of the filter parameters. On the basis of the parameter study it is suggested to use a filter radius of 20 pixels, a cut-off distance of five pixels and a filter order of $n = 3$ for domains with a side length of 200 pixels. This parameter setup has been shown to be the most reliable combination of filter parameters.

3.2. Comparison between the FTMA-method and the MFIA-method

The comparison between the FTMA-method and the MFIA-method is based on several software generated micrographs with varying mean orientations and standard deviations. The results of

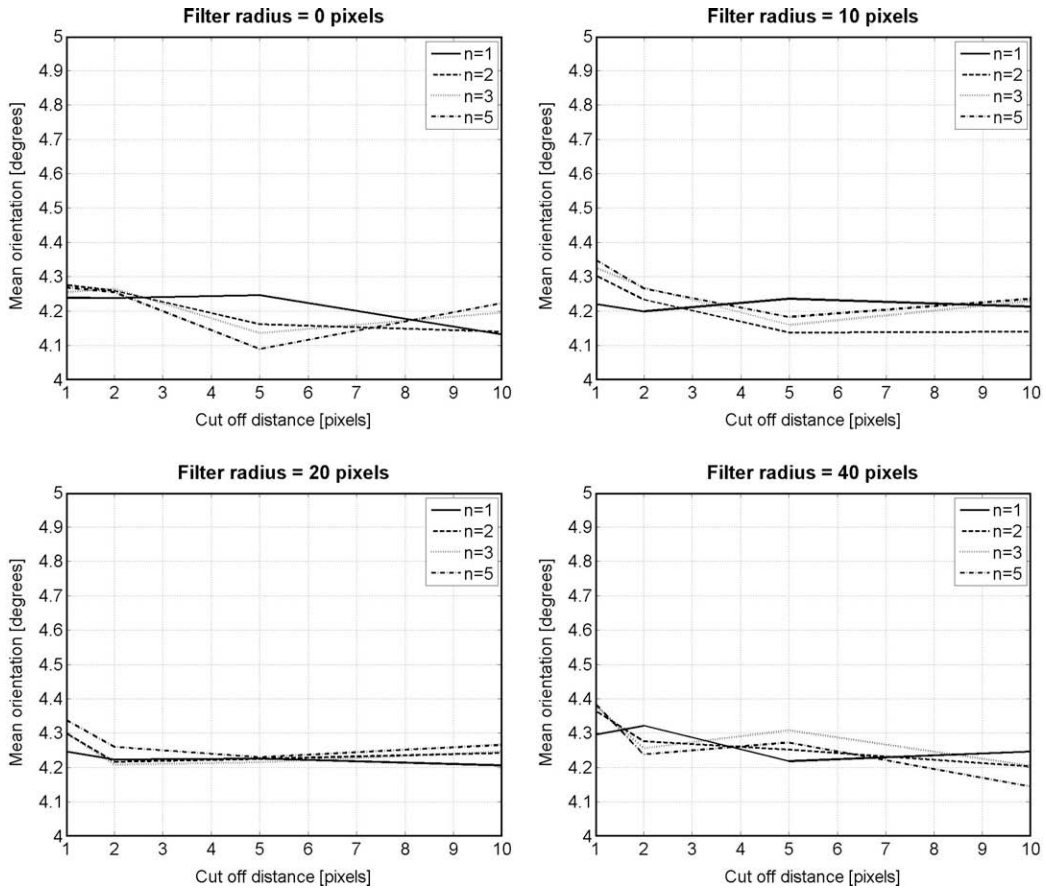

Fig. 18. Investigation of how the filter parameters influence the computation of the mean orientation. Each graph represents a filter radius, each line style the order of the filter, the cut-off distance is shown along the *x*-axis and the computed mean orientation is shown along the *y*-axis.

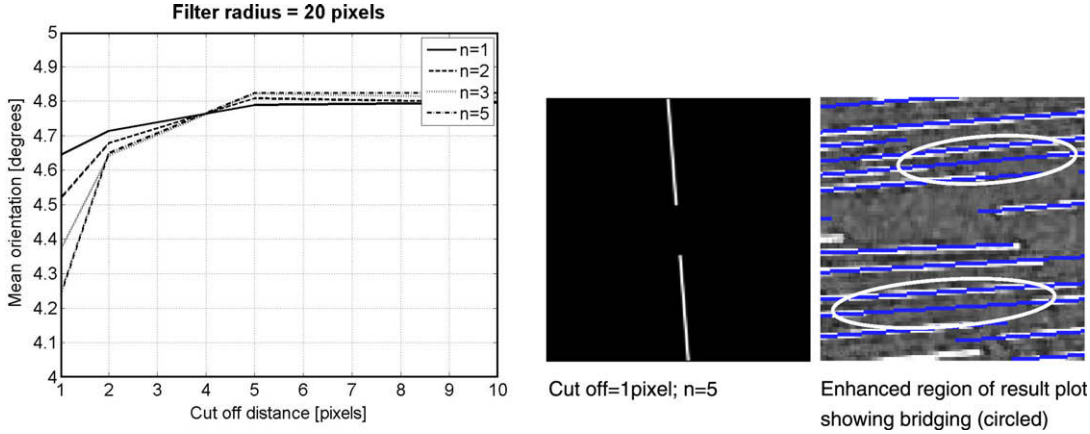

Fig. 19. Parameter investigation on software generated micrograph. The filter uses a cut-off distance of one pixel and a filter order of $n = 5$. The corresponding results plot shows examples of bridging between independent fibres (circled).

the benchmark test exploring the precision of the mean orientation and standard deviation estimates for the fibre misalignment is shown in Fig. 21.

If the precision depends on the nominal orientation, this must be considered when capturing the digital micrographs. The results shown in Fig. 21a clearly show that the precision of determining the mean orientation is not influenced significantly by the nominal orientation itself. The two methods have equal precision below ±0.1°.

When computing the standard deviation the precision of the two methods are quite different, as seen in Fig. 21b. The MFIA is relatively imprecise regarding the determination of the standard deviation. The FTMA-method has a precision below ±0.1° for standard deviations up to 3°.

The efficiency of the FTMA-method and the modified MFIA-methods has been determined under the same conditions on a laptop with a 1.86 GHz Pentium M processor and 1.5 GB RAM. The efficiency in terms of computation time of the FTMA-method and the modified MFIA-method is shown in Fig. 22.

The FTMA-method is, as Fig. 22 shows, significantly faster than the MFIA-method. Both the modified MFIA-method and the FTMA-method can now perform a typical analysis with 100 domains of

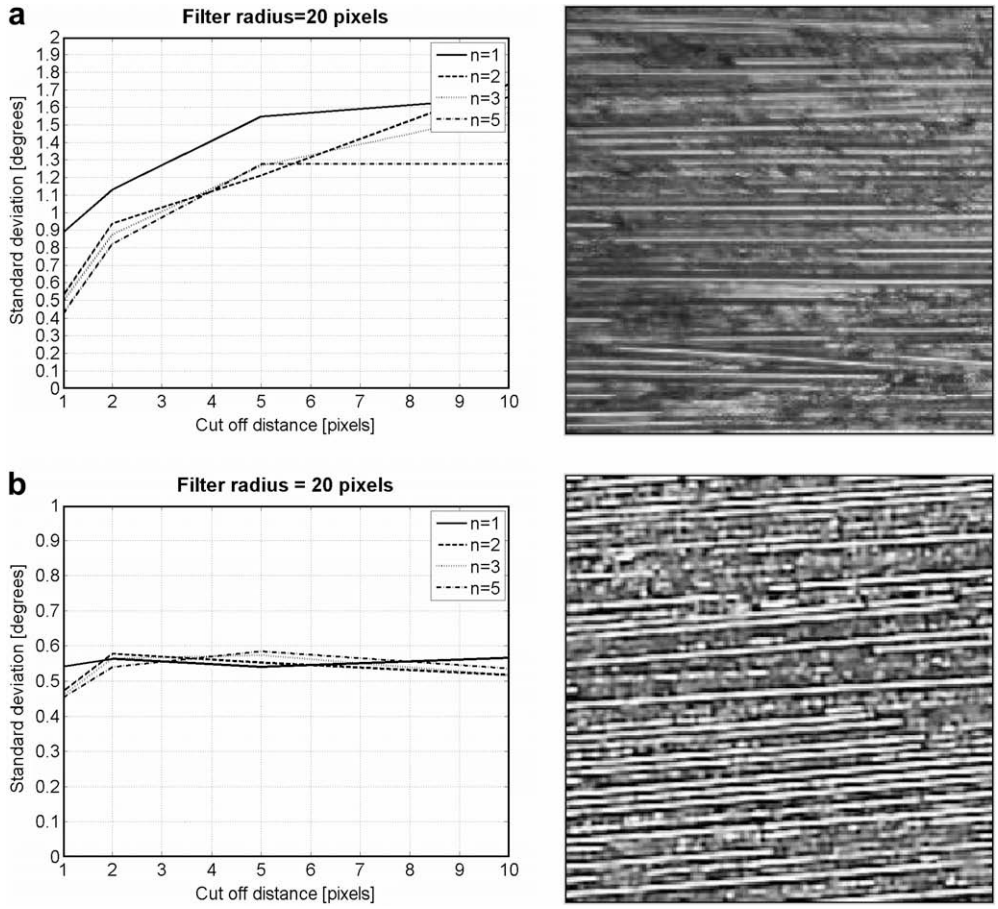

Fig. 20. Parameter investigation with a focus on the variation of the computed standard deviation: (a) with extreme variations and (b) with low variations.

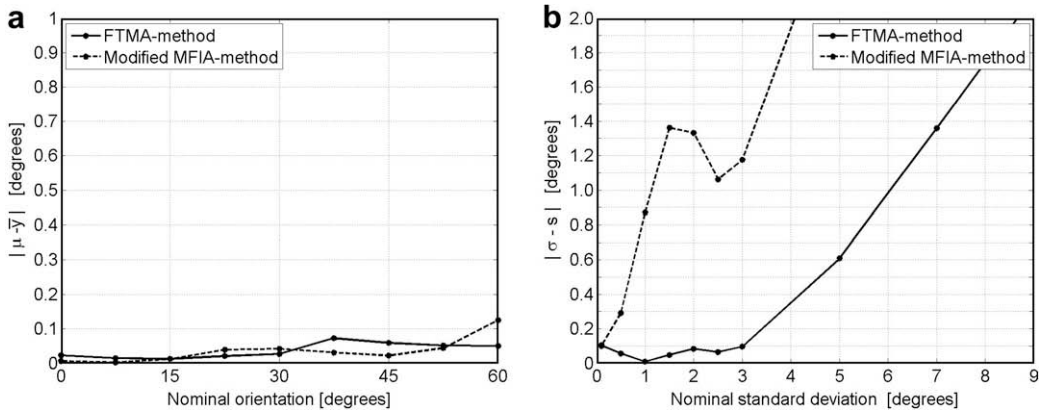

Fig. 21. (a) The absolute difference between the known mean orientation μ and the estimated mean $\bar{y}$. (b) The absolute difference between the known standard deviation σ and the estimated standard deviation s.

200 by 200 pixels in less than 5 min. However, the FTMA-method is 4–5 times faster than the MFIA-method.

As mentioned in Section 2.2 the cost of making the MFIA-method more efficient in terms of computation time is an increased memory usage. The increased memory usage of the modified MFIA-method compared to the FTMA-method is shown in Fig. 23.

The efficiency of the modified MFIA-method and the FTMA-method is summarised in Table 1.

4. Conclusions

A novel method for determining the fibre misalignment in unidirectional composite materials using 2D fast Fourier transformation has been proposed. A parameter study on both real and software generated fibre distribution micrographs has been performed to demonstrate the robustness of the FTMA-method. The results obtained have been shown to give an estimate of the mean orientation consistent within ±0.2°, independent of the filter

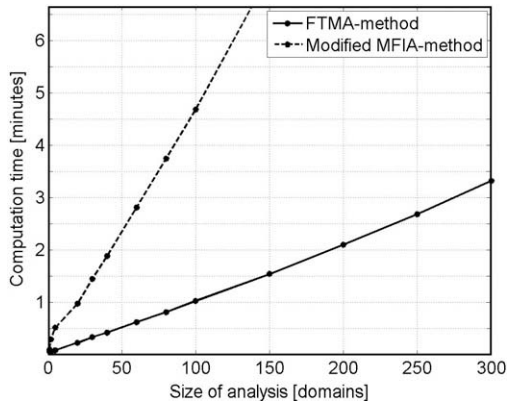

Fig. 22. Computation time of the modified MFIA-method and the FTMA-method. The size of the analysis is given in domains which have a size of 200 by 200 pixels.

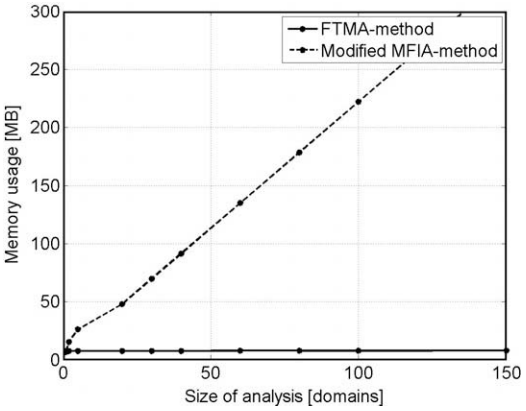

Fig. 23. Memory usage for the modified MFIA-method and the FTMA-method as a function of the size of the analysis in terms of number of 200 by 200 pixel domains. The modified MFIA increases memory usage because it analyses all domains simultaneously in order to reduce computation time.

Table 1
Benchmark of the modified MFIA-method and the FTMA-method.

1.86 GHz Pentium M processor 1.5 GB RAM 200 by 200 pixels domains	FTMA	Modified MFIA
Precision		
Nominal orientation	0.1°	0.1°
Standard deviation	0.1°	–
Time efficiency (100 domains)	1 min	4.5 min
Memory usage (100 domains)	8 MB	>200 MB

parameters. The parameter study, however, also indicates that the robustness of the computed standard deviation is influenced by the quality of the micrograph and thereby indirectly by the polishing quality when preparing the composite specimens. Fast polishing techniques therefore need to be developed further in order to increase the polishing quality and thereby improve the robustness of the computation of misalignment within a domain.

The precision of the FTMA-method has been estimated by the use of software generated micrographs. These show that both the MFIA-method and the FTMA-method have a precision in estimating the mean fibre orientation better than ±0.1°. With software generated micrographs with randomly distributed fibre misalignment the FTMA-method displays a uniform precision for standard deviations below 3°. The MFIA-method, however, is not able of capturing the fibre misalignment when it is randomly distributed. This is an important advantage of the FTMA-method as this was reported by Liu et al. [18] to be an important factor governing the compression strength of composite laminates.

The FTMA-method has been applied to the analysis of the fibre misalignment of several unidirectional CFRP laminates manufactured by pultrusion or using prepregs. Comparing with the original MFIA-method, the modified MFIA-method used in this paper is significantly faster. The largest time reduction, from the reported 3 h to approximately 15 min, is given by the increased efficiency of computers. The last reduction in computation time from 15 min to approximately 5 min for the MFIA-method can be obtained by analysing all domains simultaneously. The FTMA-method, however, remains a factor of 4–5 faster than the modified MFIA-method.

Acknowledgements

The work presented has been conducted as part of an industrial Ph.D. program carried out in close collaboration between Fiberline Composites A/S, Middelfart, Denmark and the Department of Mechanical Engineering, Aalborg University, Denmark. Moreover, a substantial part of the work reported herein connected to the so-called MFIA-method for the analysis of fibre misalignment in composite laminates was conducted during a 1 month visit of the first author with the Department of Engineering, University of Cambridge, UK. The kind hospitality of the Department of Engineering, University of Cambridge and access to its experimental and modelling facilities is gratefully acknowledged.

References

[1] Budiansky B, Fleck NA. Compressive failure of fibre composites. J Mech Phys Solids 1993;41:183–211.
[2] Budiansky B, Fleck NA. Compressive failure of fibre composites due to microbuckling. Inelastic deformation of composite materials, IUTAM symposium; 1991. p. 236–74.
[3] Yurgartis SW. Measurement of small angle fiber misalignments in continuous fiber composites. Compos Sci Technol 1987;30:279–93.
[4] Clarke AR, Archenhold G, Davidson NC. A novel technique for determining 3D spatial distribution of glass fibres in polymer composites. Compos Sci Technol 1995;55:75–91.
[5] Clarke AR, Archenhold G, Davidson NC, Fleck NA. Determining the power spectral density of the waviness of unidirectional glass fibres in polymer composites. Appl Compos Mater 1995;2:233–43.
[6] Creighton CJ, Sutcliffe MPF, Clyne TW. A multiple field image analysis procedure for characterisation of fibre alignment in composites. Compos Part A: Appl Sci Manuf 2001;32:221–9.
[7] Homepage: <http://rsb.info.nih.gov/ij/>.
[8] Gonzalez RC, Woods RE. Digital image processing. 2nd ed. Prentice Hall; 2002 [ISBN: 0-130-94650].
[9] Rosen BW. Strength of uniaxial fibrous composites. Mech Compos Mater 1970:621–51.
[10] Sutcliffe MPF. Micromechanics and compressive loading of composite materials. In: Proceedings of the 27th Risø international symposium, 2006. p. 48–68.
[11] Drapier S, Grandidier J, Potier-Ferry M. Theoretical study of structural effects on the compressive failure of laminate composites. CR Acad Sci, Ser IIB – Mech, Phys, Chem, Astron 1997;324:219–27.
[12] Fleck N. Compressive failure of fibre composites. Adv Appl Mech 1997;33:43–119.
[13] Argon AS. Fracture of composites. Treatise on material science and technology, vol. 1. New York: Academic Press; 1972. p. 79-114.
[14] Budiansky B. Micromechanics. Comput Struct 1983;16:3–12.
[15] Wisnom MR. The effect of fibre misalignment on the compressive strength of unidirectional carbon fibre/epoxy. Composites 1990;21:403–7.
[16] Kyriakides S, Arseculeratne R, Perry EJ, Liechti KM. On the compressive failure of fiber reinforced composites. Int J Solids Struct, Time Dependent Problems Mech 1995;32:689–738.
[17] Fleck NA, Shu JY. Microbuckle initiation in fibre composites: A finite element study. J Mech Phys Solids 1995;43:1887–918.
[18] Liu D, Fleck NA, Sutcliffe MPF. Compressive strength of fibre composites with random fibre waviness. J Mech Phys Solids 2004;52:1481–505.